BIOCHEMISTRY
including biophysical chemistry & molecular biology

Article

pubs.acs.org/biochemistry

Mutational Analysis of the C8-Guanine Adduct of the Environmental Carcinogen 3-Nitrobenzanthrone in Human Cells: Critical Roles of DNA Polymerases η and κ and Rev1 in Error-Prone Translesion Synthesis

Paritosh Pande, Chanchal K. Malik, Arindam Bose, Vijay P. Jasti, and Ashis K. Basu*

Department of Chemistry, University of Connecticut, Storrs, Connecticut 06269, United States

Supporting Information

ABSTRACT: 3-Nitrobenzanthrone (3-NBA), a potent mutagen and suspected human carcinogen, is a common environmental pollutant. The genotoxicity of 3-NBA has been associated with its ability to form DNA adducts, including *N*-(2′-deoxyguanosin-8-yl)-3-aminobenzanthrone (C8-dG-ABA). To investigate the molecular mechanism of C8-dG-ABA mutagenesis in human cells, we have replicated a plasmid containing a single C8-dG-ABA in human embryonic kidney 293T (HEK293T) cells, which yielded 14% mutant progeny. The major types of mutations induced by C8-dG-ABA were G → T > G → A > G → C. siRNA knockdown of the translesion synthesis (TLS) DNA polymerases (pols) in HEK293T cells indicated that pol η, pol κ, pol ι, pol ζ, and Rev1 each have a role in replication across this adduct. The extent of TLS was reduced with each pol knockdown, but the largest decrease (of ∼55% reduction) in the level of TLS occurred in cells with knockdown of pol ζ. Pol η and pol κ were considered the major contributors of the mutagenic TLS, because the mutation frequency (MF) decreased by 70%, when these pols were simultaneously knocked down. Rev1 also is important for mutagenesis, as reflected by the 60% reduction in MF upon Rev1 knockdown, but it probably plays a noncatalytic role by physically interacting with the other two Y-family pols. In contrast, pol ζ appeared to be involved in the error-free bypass of the lesion, because MF increased by 60% in pol ζ knockdown cells. These results provide important mechanistic insight into the bypass of the C8-dG-ABA adduct.

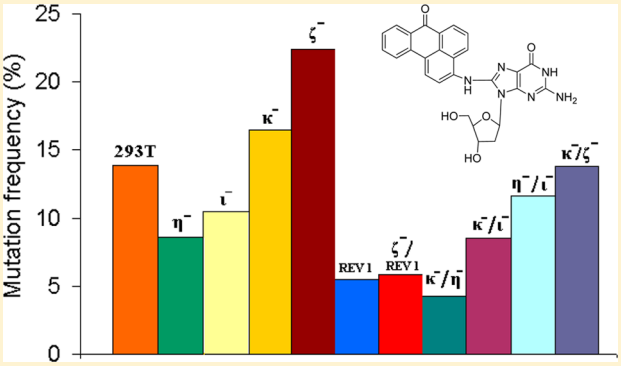

Nitroaromatic compounds, of which many are mutagens and human carcinogens, are common environmental pollutants.[1] In 1997, 3-nitrobenzanthrone (3-NBA), an aromatic nitroketone, was first reported to be present in diesel exhaust and airborne particulates.[2] 3-NBA is one of the most potent mutagens in the Ames *Salmonella typhimurium* assay.[2,3] It is also highly mutagenic in mammalian cells. 3-NBA's genotoxicity in mammalian cells was shown by induction of micronuclei in mouse peripheral blood reticulocytes, human B-lymphoblastoid cells, and human hepatoma cell lines.[4−7] 3-NBA induces lung tumors in experimental animals and is a suspected human carcinogen.[8] The carcinogenicity of 3-NBA is as potent as that of the powerful carcinogen 1,6-dinitropyrene in F344 rats.[9]

Like many other nitropolycyclic aromatic hydrocarbons, 3-NBA is metabolically activated by cellular nitro reduction to form an *N*-hydroxy arylamine, which can either form a nitrenium ion or undergo metabolic esterification to generate highly electrophilic derivatives that form DNA adducts.[1,10−12] The primary stable metabolite of 3-NBA in mammalian cells is 3-aminobenzanthrone, which was detected in workers occupationally exposed to diesel exhaust.[13] Three major DNA adducts of 3-NBA detected in cells and tissues of exposed animals are *N*-(2′-deoxyguanosin-8-yl)-3-aminobenzanthrone (C8-dG-ABA), 2-(2′-deoxyguanosin-N^2-yl)-3-aminobenzanthrone (N^2-dG-ABA), and 2-(2′-deoxyadenosin-N^6-yl)-3-aminobenzanthrone (N^6-dA-ABA) (Scheme 1).[14] Both the high initial level of the DNA adducts and their persistence in target organs such as lung suggest an association of these lesions with the carcinogenic effect of 3-NBA.[9,15] Most mutations caused by 3-NBA in experimental animals occur in guanine residues, inducing primarily GC → TA transversions.[15] Replication of a plasmid treated with *N*-acetoxy-3-aminobenzanthrone, a major reactive metabolite of 3-NBA, provided predominantly G → T base substitutions followed by G → A and A → G mutations.[16]

Bulky DNA adducts such as those formed by 3-NBA are known to be strong blocks of replicative DNA polymerases (pols).[17,18] When DNA replication stalls, a group of specialized DNA pols takes over replication across these lesions, and this process is termed translesion synthesis (TLS).[19−24] The TLS

Received: June 24, 2014
Revised: July 21, 2014
Published: July 31, 2014

   dx.doi.org/10.1021/bi5007805 | *Biochemistry* 2014, 53, 5323−5331

Scheme 1. Chemical Structures of 3-NBA and Its Major DNA Adducts

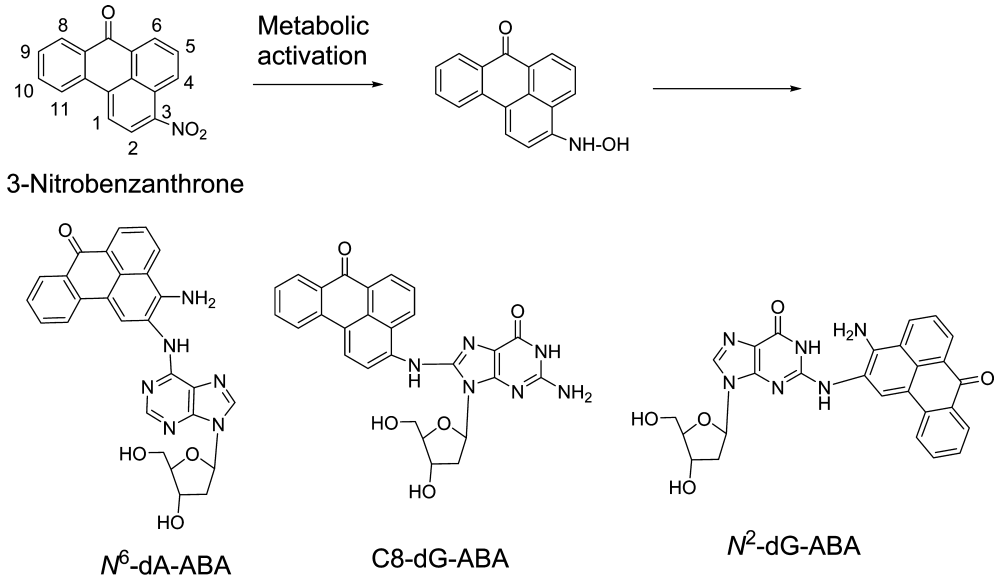

pols are structurally better equipped to bypass the DNA lesions, but they replicate undamaged DNA with a rate of errors higher than that of replicative pols. The discovery of the TLS pols has triggered intense research in the past two decades to improve our understanding of the mechanism of both spontaneous and lesion-induced mutagenesis as well as their link to the etiology of cancer.[25,26] Because DNA lesions have a wide variety of structures and shapes, there is no unified mechanism of TLS; nevertheless, certain patterns of TLS have been observed for specific DNA lesions.[27] In eukaryotic cells, efficient lesion bypass is achieved cooperatively by two sequential steps.[28−31] In the first step, one of the TLS pols inserts a nucleotide opposite the DNA lesion. In the subsequent step, the insertion pol is replaced by another TLS pol to conduct primer extension past the lesion site. Certain accessory proteins are also critical for TLS.[32−36] However, many questions, including how these TLS pols are selected and recruited for a particular lesion and how the switch among different pols is coordinated, remain unanswered at present. In mammalian cells, TLS is conducted by pol η, pol κ, pol ι, and Rev1 of the Y-family pols and pol ζ of the B-family enzymes.[31,37,38] Pol η is unique in its ability to promote proficient and error-free bypass of UV-induced cyclobutane pyrimidine dimers, although it incorporates wrong nucleotides at a high rate opposite several other lesions.[39,40] Pol η also slowly bypasses the C8-dG-2-amino-fluorene and its acetylated analogue predominantly in an error-free manner.[41] It was suggested that the TLS efficiency of pol η depends on the size of the bulky adduct. In this proposed model, TLS is accomplished without rotation of the lesion into the *anti* conformation.[41] In a similar vein, pol κ bypasses the (+)-*trans*-BPDE-N^2-dG adduct and other N^2-dG adducts with efficiency and accuracy reasonably high compared to those of other TLS pols.[42−45] Pol κ and pol ζ together promote error-free replication through oxidative DNA damage, *cis*-thymine glycol.[46] For several other lesions, however, pol κ was suggested to catalyze the extension step.[40,47] In contrast to pol η and pol κ, which select the incoming dNTP based on Watson−Crick base pairs, pol ι utilizes Hoogsteen base pairs with the template base,[48,49] yet in the only reported crystal structure of a bulky C8-dG adduct of 1-nitropyrene complexed with pol ι at the insertion stage, the adduct was determined to be in its active site in two distinct conformations.[50] dCTP forms a Watson−Crick base pair with the adducted guanine and excludes the pyrene ring from the helical DNA, which inhibits replication beyond the lesion. In contrast, the mismatched dATP stacks above the pyrene ring intercalated in the helix, so that the pyrene mimics a base pair in the active site and facilitates adenine misincorporation by pol ι.

The roles of various TLS polymerases in bypassing the 3-NBA-DNA adducts have not yet been studied. A goal of this work is to explore the functions of various TLS pols in bypassing the C8-dG-ABA adduct in both an error-free and an error-prone manner. We present here the results of our investigation of the molecular mechanism of mutagenesis by C8-dG-ABA in human embryonic kidney 293T (HEK293T) cells, in which the siRNA knockdown approach was employed to identify the TLS pols and to determine their roles in replication across this adduct.

MATERIALS AND METHODS

Materials. All starting materials, reagents, and solvents were of commercial grade and used as such unless otherwise specified. [γ-^{32}P]ATP was from Du Pont New England Nuclear (Boston, MA). *Eco*RV restriction endonuclease, T4 DNA ligase, T4 polynucleotide kinase, uracil DNA glycosylase, and exonuclease III were obtained from New England Bioloabs (Beverly, MA). Plasmid pMS2 was a gift from M. Moriya (Stony Brook University, The State University of New York, Stony Brook, NY). HEK293T/17 and COS-7 cells were purchased from the American Type Culture Collection (Manassas, VA).

siRNAs. Synthetic siRNA duplexes against PolH (SI02663619), PolK (SI04930884), PolI (SI03033310), Rev1 (SI00115311), and AllStars Negative control siRNA (1027280) were purchased from Qiagen (Valencia, CA), whereas the same for Rev3 was purchased from Integrated DNA Technologies (Coralville, IA). Sequences of all the siRNAs are listed in Table S1 of the Supporting Information.

Methods. *Construction and Characterization of a pMS2 Vector Containing a Single C8-dG-ABA.* We constructed a single adduct-modified single-stranded vector, pMS2, with

dx.doi.org/10.1021/bi5007805 | *Biochemistry* 2014, 53, 5323−5331

neomycin and ampicillin resistance genes, as follows.[51] The pMS2 DNA (58 pmol, 100 μg) was digested with an excess of *Eco*RV (300 pmol, 4.84 μg) for 1 h at 37 °C and then at room temperature overnight. A 58-mer scaffold oligonucleotide was annealed overnight at 9 °C to form the gapped DNA template. The 12-mer containing C8-dG-ABA, 5′-GTGCG*TGTTTGT-3′, was synthesized as described previously.[52] The adducted 12-mer was purified by reverse-phase high-performance liquid chromatography followed by denaturing polyacrylamide gel electrophoresis and was analyzed by mass spectrometry (Figures S1 and S2 of the Supporting Information). The control and C8-dG-ABA-containing oligonucleotides were phosphorylated with T4 polynucleotide kinase, hybridized to the gapped pMS2 DNA, and ligated overnight at 16 °C. Unligated oligonucleotides were removed by being passed through a Centricon-100 apparatus, and the DNA was precipitated with ethanol. The scaffold oligonucleotide was digested by treatment with uracil DNA glycosylase and exonuclease III; the proteins were extracted with phenol and chloroform, and the DNA construct was precipitated with ethanol. The final construct was dissolved in 1 mM Tris-HCl and 0.1 mM EDTA (pH 8), and a portion was subjected to electrophoresis on a 1% agarose gel to assess the amount of circular DNA, which established that at least 40% ligation of the 12-mers occurred on both sides of the gap.

Replication and Analysis in Human Embryonic Kidney (HEK293T) Cells. The HEK293T/17 cell line is a derivative of the 293T cell line (293tsA1609neo).[53] It is a highly transfectable derivative of the 293 cell line into which the temperature sensitive gene for simian virus 40 (SV40) T antigen was inserted. These cells constitutively express the SV40 large T antigen. The 293T/17 cells were maintained in Dulbecco's modified Eagle's medium supplemented with 4 mM L-glutamine and adjusted to contain 1.5 g/L sodium bicarbonate, 4.5 g/L glucose, and 10% fetal bovine serum. The cells were grown to ∼90% confluency and transfected with 50 ng of each construct using 6 μL of Lipofectamine cationic lipid reagent (Invitrogen, Carlsbad, CA). Following transfection with modified or unmodified pMS2, the cells were allowed to grow at 37 °C in 5% CO_2 for 2 days, and then the plasmid DNA was collected and purified by the method of Hirt.[54] It was then used to transform *Escherichia coli* DH10B, and transformants were analyzed by oligonucleotide hybridization. Oligonucleotide probes containing the complementary 16-mer sequence were used to analyze progeny plasmids. The 14-mer left and 15-mer right probes were used to select plasmids containing the correct insert, and transformants that did not hybridize with both the left and right probes were omitted. Any transformant that hybridized with the left and right probes but failed to hybridize with the 16-mer wild-type probe was subjected to DNA sequence analysis.

Replication and Analysis in Simian Kidney Cells. COS-7 cells were grown in Dulbecco's modified Eagle's medium supplemented with 10% fetal bovine serum. The cells were seeded at a density of 5×10^5 cells per 60 mm plate. Following overnight incubation, the cells were transfected with 50 ng of single-stranded DNA by electroporation or using 6 μL of Lipofectamine cationic lipid reagent (Invitrogen, Carlsbad, CA). The culture was incubated for 2 days, and the progeny plasmid was recovered by the method of Hirt.[54] Subsequent transformation in *E. coli* DH10B and analysis were performed in a manner similar to that used with the plasmid from HEK293T cells.

TLS Assay in Human Cells. The lesion-containing or control pMS2 construct was mixed with equal amount of a single-stranded pMS2 DNA containing the same DNA sequence as the construct except it contained a C in place of G two nucleotides 5′ to the lesion site (i.e., 5′-GTCCGTGTTTGT-3′). The mixed DNA was used to transfect HEK293T cells and processed as described above. Oligonucleotide probes for the complementary sequences for both the wild type and the mutant plasmid were used to analyze the progeny. The mutant DNA was used as an internal control, and it gave the same number of progeny as the control construct. Typically, three independent experiments were performed to determine the extent of TLS with each pol knockdown.

Mutational Analyses of TLS Products from Human Cells with Pol Knockdowns. Prior to transfection of the control and C8-dG-ABA-containing vectors, synthetic siRNA duplexes were transfected into HEK293T cells using Lipofectamine. HEK293T cells were plated in six-well plates at 50% confluence. After being incubated for 24 h, they were transfected with 100 pmol of the siRNA duplex mixed with Lipofectamine, diluted in Opti-MEM (Gibco), per well. One day before the transfection of the plasmid, cells were seeded in 24-well plates at 70% confluence. Cells were then cotransfected with another aliquot of siRNA and either the control plasmid or the lesion-containing plasmid at a ratio of 2:1. After being incubated for 24 h, progeny plasmids were isolated as described above.

Reverse Transcription Polymerase Chain Reaction (RT-PCR) Analysis. Total RNA was extracted from the cells 72 h after the first transfection of siRNA duplexes, using the All Prep DNA/RNA/Protein Kit (Qiagen). One hundred nanograms of total RNA was used for RT-PCR analysis, performed with the One Step RT-PCR Kit (Qiagen) according to the manufacturer's instructions. Primer sequences used for RT-PCR are listed in Table S2 of the Supporting Information. Using primers specific to TLS DNA polymerases and control gene GAPDH, the siRNA knockdown efficiency was determined as previously described.[39] Reverse transcription and the PCR initial activation step were performed for 30 min at 50 °C and 15 min at 95 °C, respectively. For PolH, PolK, PolI, and Rev1, amplification was conducted at 94 °C for 30 s, 55 °C for 45 s, and 72 °C for 60 s for 26 cycles and Rev3 was amplified for 32 cycles. Amplification of GAPDH was conducted at 94 °C for 30 s, 55 °C for 45 s, and 72 °C for 45 s for 24 cycles. RT-PCR products were analyzed on a 2% agarose gel run at 100 V for 3 h in 1× TBE buffer.

Western Blotting. Cells were washed with cold phosphate-buffered saline and collected into a chilled Eppendorf tube. They were lysed in ice-cold RIPA buffer (Sigma-Aldrich, St. Louis, MO) containing protease inhibitor cocktail (Roche, Indianapolis, IN) and incubated for 1 h on ice, and the mixture was centrifuged at 10000 rpm for 15 min at 4 °C. The supernatant was used for the determination of the protein concentration by the Bradford assay and for Western blotting. The protein extracts (40 μg of each whole cell lysate) were boiled in loading sample buffer [250 mM Tris (pH 6.8), 5% sodium dodecyl sulfate, 30% glycerol, 20% β-mercaptoethanol, and bromophenol blue]. Proteins were separated on either 5 or 7% sodium dodecyl sulfate−polyacrylamide gel electrophoresis gels by electrophoresis for 2 h and transferred onto polyvinylidene fluoride membranes (Bio-Rad Laboratories, Hercules, CA). The membranes were blocked with 5% milk and then incubated with antibodies that specifically recognize

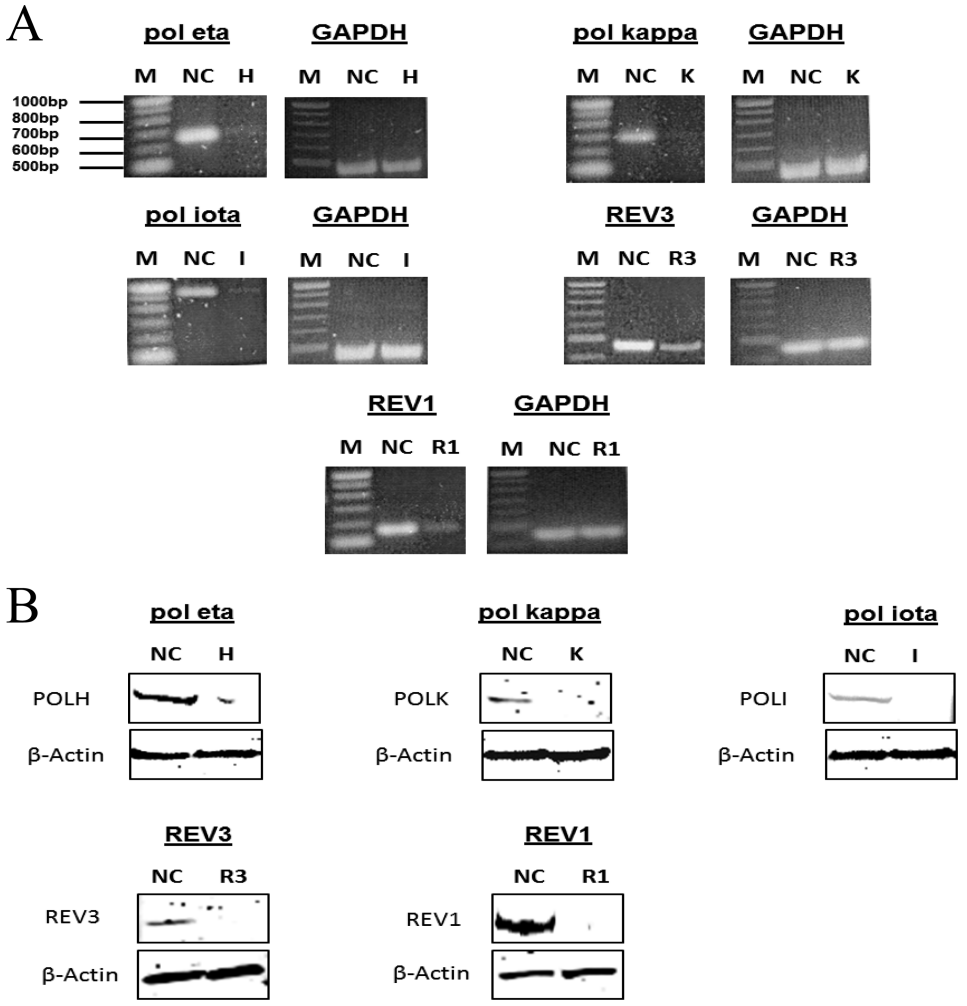

Figure 1. (A) Representative gel images of siRNA knockdown of TLS pols in HEK293T cells. RT-PCR shows the efficiency of inhibition of TLS pols: M, DNA size marker; NC, negative control siRNA; H, pol η; K, pol κ; I, pol ι; R3, Rev3 of pol ζ; R1, Rev1. In each case, as a negative control of RT-PCR, the effects of siRNA on glyceraldehyde-3-phosphate dehydrogenase (GAPDH) mRNA expression were also examined. (B) Western blot analysis of the siRNA knockdown of TLS pols in HEK293T cells 48 h after siRNA transfection. After the isolation of cellular extracts, target protein expression was analyzed by Western blotting.

human PolH (Pierce, Rockford, IL), PolK, PolI, Rev3, or Rev1 (Santa Cruz Biotechnology, Santa Cruz, CA). The human β-actin antibody (Sigma-Aldrich) was used to confirm equal gel loading. Horseradish peroxidase-conjugated goat anti-rabbit (Sigma-Aldrich) and goat anti-mouse (Santa Cruz Biotechnology) antibodies were used at 1:5000 dilutions. The signals were developed using Pierce ECL Western Blotting Substrate (Thermo Scientific, Rockford, IL), and the images were taken using a PhosphorImager.

RESULTS

Contribution of Pols η, κ, ι, and ζ and Rev1 in TLS of C8-dG-ABA. To determine the roles of the TLS polymerases in replicating across C8-dG-ABA, we employed a siRNA knockdown approach to constrain their expression. The extent of siRNA knockdown was determined by RT-PCR (Figure 1A) and by Western blotting analysis (Figure 1B). For each pol, the knockdown was at least 70% efficient. HEK293T cells were first transfected with siRNA for 48 h to reduce the level of expression of the TLS pol. Subsequently, another aliquot of siRNA and a mixture of the lesion-containing construct and unmodified plasmid DNA were cotransfected into these cells. The unmodified DNA contained a C instead of G two nucleotides 5′ to the lesion site, so that it could be used as an internal control. Cells were incubated for 24 h to allow for the replication of the plasmids, which were isolated and used to transform *E. coli* DH10B cells. The percentages of the colonies originating from the lesion-containing plasmid relative to the unmodified mutant plasmid, reflecting the percentage of TLS, were determined by oligonucleotide hybridization. In HEK293T cells, in which no pol was knocked down but the cells were also transfected with negative control (NC) siRNA, the frequency of TLS was 74% for the C8-dG-ABA-containing plasmid relative to 100% progeny generated from the undamaged plasmid (Figure 2). This is similar to the reported TLS efficiency of dG-N^2-AAF and dG-C8-AAF adducts transfected in COS-7 cells,[55] but for knockdown of each of the pols, there was a reduction in the level of progeny from the C8-dG-ABA plasmid (Figure 2). Knockdown of Rev3 of pol ζ resulted in the largest reduction (>50%) in TLS efficiency to give ~35% progeny, whereas knockdown of pol ι provided a reduction of ~20% relative to the same from NC-siRNA-treated (or untreated) cells (Figure 2). Knockdown of pol η or κ or Rev1 gave intermediate values of TLS efficiency (Figure 2).

dx.doi.org/10.1021/bi5007805 | *Biochemistry* 2014, 53, 5323−5331

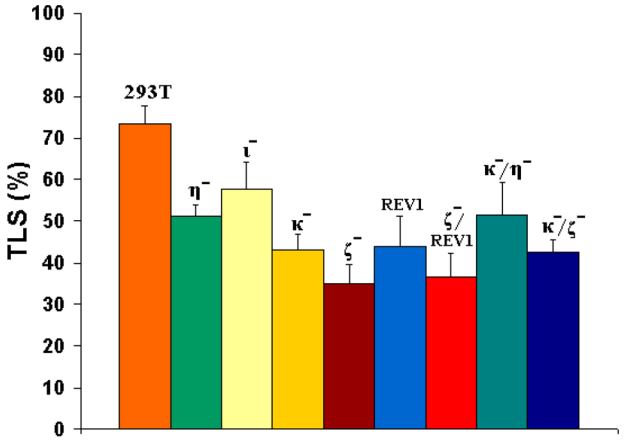

Figure 2. Effects of siRNA knockdowns of TLS pols on the extent of replicative bypass of C8-dG-ABA. The percent TLS in various pol knockdowns was measured using an internal control of an unmodified plasmid containing a mutation two nucleotides 5′ to the lesion site. The data represent the means and standard deviations of results from three independent experiments (except in the knockdown experiment with pol κ and pol ζ that was performed twice). HEK293T cells were treated with negative control (NC) siRNA, whereas the other single- or double-pol knockdowns are indicated above the bar. The TLS result from each knockdown experiment was considered statistically significant ($p < 0.05$) compared to that from HEK293T cells treated with NC siRNA. The p value of TLS efficiency for each knockdown was calculated by using a two-tailed, unpaired Student's t test.

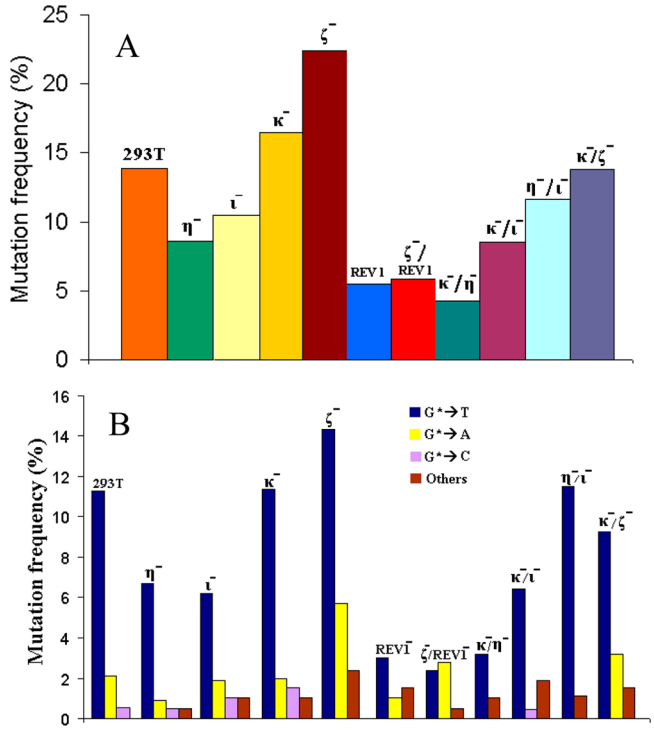

Figure 3. Mutational frequency of C8-dG-ABA in HEK293T cells also transfected with NC siRNA (293T) or siRNA for single- or double-pol knockdowns shown above the bar. The data represent the average of two independent experiments (shown in Table S4A–K of the Supporting Information). Panel A shows the total MFs (%) in various TLS pol knockdowns, whereas panel B shows the types of mutations in each case.

However, for the two-polymerase knockdown experiments, involving pol ζ and Rev1, pol η and pol κ, or pol κ and pol ζ, the TLS efficiency of the C8-dG-ABA adduct did not change appreciably for the lack of a second pol (Figure 2). These results suggest that each TLS pol plays a role in bypassing C8-dG-ABA; yet none of them are essential for TLS of C8-dG-ABA. It also seems likely that the TLS pols can compensate for the absence of one or two pols to replicate past the lesion.

Mutational Specificity of C8-dG-ABA in HEK293T Cells. DNA sequence analysis of the TLS products showed that 86% bypass in HEK293T cells, also transfected with NC siRNA, occurred in an error-free manner, and only 14% were mutants (Figure 3A). Mutations were analyzed for two independently constructed vectors, and though mutagenesis data (provided in Table S4 of the Supporting Information) were consistent in the two transfections, combined data from the two experiments are presented in panels A and B of Figure 3 for ease of analysis. The fact that the TLS polymerases play critical roles in C8-dG-ABA mutagenesis is clearly evident from Figure 3A. MF decreased with pol η, pol ι, or Rev1 knockdown, whereas it increased with pol κ or pol ζ knockdown. In the single-pol knockdown experiments, knockdown of pol η caused a 39% reduction in MF, compared to a 28% reduction in MF with pol ι knockdown (Figure 3A). However, the largest decrease in MF occurred with Rev1 knockdown, when it was reduced by 61% (Figure 3A). Rev1 acts as a scaffold that interacts with the Rev1-interacting region of pol η, κ, and ι,[56] and our result suggests a critical role of Rev1 in C8-dG-ABA mutagenesis. In contrast, MF increased by 60% when pol ζ was knocked down. Because pol ζ has been reported to be an extender after incorporation of a nucleotide opposite the lesion,[57] it is conceivable that pol ζ preferentially extends the G*:C base pair following the incorporation of the correct dCMP by other TLS pols. Interestingly, simultaneous knockdown of pol ζ and Rev1 produced the same level of MF as Rev1 knockdown (Figure 3A). A modest 15% increase in MF occurred with knockdown of pol κ, which was also reported to act as an extender for several DNA lesions.[40,58,59] Remarkably, simultaneous knockdown of pol η and pol κ resulted in the largest (~70%) reduction in MF (Figure 3A), which suggests that these two pols play critical functions in the mutagenic TLS of C8-dG-ABA, but two-pol knockdown of pol κ and pol ι or of pol η and pol ι showed no synergistic effect and exhibited MF between the MFs from the single knockdown of each pol (Figure 3A). The major types of mutations by C8-dG-ABA in HEK293T cells were G → T mutations followed by G → A mutations, but a low level of G → C and semitargeted mutations also occurred (Figure 3B). The most common semitargeted mutation at the 5′ base adjacent to C8-dG-ABA was the C → T mutation, but C → G and C → A mutations also were detected in some cases (Table S4 of the Supporting Information and Figure 3B). It is important to point out that for the control construct, no mutations were detected within the 12-mer sequence in approximately 300 progeny that were analyzed.

While this work was in progress, a research article on the formation and repair of 3-NBA-treated cells and translesion synthesis past the 3-NBA adducts was published.[60] In this work, in contrast to our results, the C8-dG-ABA adduct predominantly caused G → A mutations (15.0%), followed by G → T (8.8%) and G → C (2.0%) mutations in human skin fibroblast cell line XP2OS(SV).[60] We were surprised by the change in mutational specificity between the two different human cell lines, even though an NER-deficient cell line was used in the

dx.doi.org/10.1021/bi5007805 | Biochemistry 2014, 53, 5323−5331

published work, whereas we used NER-proficient HEK293T cells. In addition to the difference in cell lines, the DNA sequence context beyond the immediate neighbors of the lesion was dissimilar in this work. Furthermore, the C8-dG-ABA adduct was located in a bubble opposite TCT in the complementary strand. We were interested in determining the effect the bubble region might have on replication of the C8-dG-ABA adduct and constructed a vector in which the scaffold contained TCT opposite C8-dG-ABA. For the sake of comparison, we also prepared a construct with a scaffold that contained C opposite the lesion. Furthermore, we decided to use a different mammalian cell line and chose simian kidney cell line COS-7. For the single-stranded C8-dG-ABA-containing vector, MF was 10.9% in COS-7 cells compared to 14% in HEK293T cells (Figure 4A). However, also in COS-7 cells, the

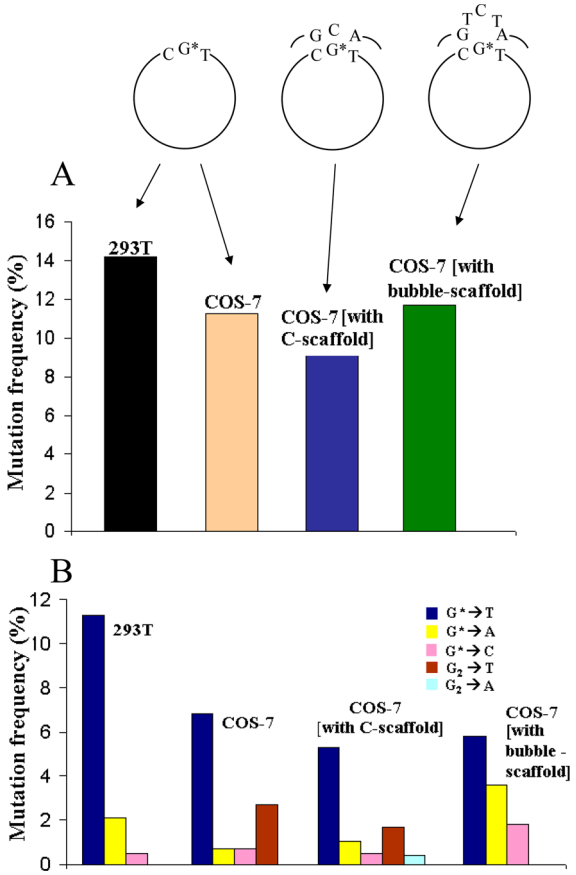

Figure 4. Comparison of MF of C8-dG-ABA in HEK293T and COS-7 cells in a single-stranded vector as well as the same in COS-7 cells when the adduct was situated opposite a C scaffold or a bubble scaffold. The data represent the average of two independent experiments (shown in Table S4A,L of the Supporting Information). Panel A shows the total MF, whereas panel B shows the types of mutations in each case.

major types of mutations were G → T mutations (6.8%), followed by G → A (0.7%) and G → C (0.7%) mutations (Figure 4B). Next, we replicated the bubble scaffold-containing plasmid in COS-7 cells, which gave >26% progeny containing the TCT sequence, a likely result of lesion repair in favor of the unmodified complementary DNA sequence. When the frame-shift progeny containing the TCT sequence were excluded, the major mutation by C8-dG-ABA was the G → T mutation (5.8%), but the G → A mutation frequency increased 5-fold to 3.7% (Figure 4B). However, when the scaffold contained a C opposite C8-dG-ABA, G → A events were less than 1% as in the single-stranded vector (Table S4L of the Supporting Information and Figure 4B). On the basis of these experiments, we conclude that the presence of C8-dG-ABA in the bubble region of the duplex plasmid, in addition to the different sequence context and the type of cells, has contributed to the array of mutations noted in ref 60.

DISCUSSION

TLS Polymerases Active in Bypassing C8-dG-ABA. Our data suggest that each TLS polymerase examined in this work, including pol η, pol κ, pol ι, and Rev1 of the Y-family pols and pol ζ of the B-family, has a role in bypassing C8-dG-ABA, as reflected by a decrease in the number of colony-forming units shown in Figure 2 with knockdown of any of these pols. However, none of them are essential for TLS. The largest decrease in TLS efficiency occurred in cells with knockdown of pol ζ (~55% reduction), followed by Rev1 or pol κ (>40% reduction). Knockdown of pol η (30% reduction in TLS) or pol ι (22% reduction in TLS) exhibited a less pronounced effect, but simultaneous knockdown of two pols did not provide a significant additional effect of the second pol. These results indicate the participation of multiple pols in TLS of C8-dG-ABA and are consistent with the current model that suggests TLS in eukaryotic cells involves two or more pols and multiple pol switches.[31,61] From an evolutionary point of view, the TLS data are also in agreement with the multiple strategies employed by the TLS pols involving Watson−Crick and non-Watson−Crick hydrogen bonding to efficiently bypass bulky lesions in DNA, such as C8-dG-ABA, which prefers to remain in a *syn* conformation.[62,63]

Error-Free versus Error-Prone TLS. Analysis of the progeny showed that replicative bypass of a C8-dG-ABA occurs in a predominantly error-free manner, as only 14% progeny contained a mutation (Figure 3). From the single-siRNA knockdown studies, we conclude that pol ζ plays a role in error-free replication, because MF was increased by 60% when pol ζ was knocked down (Figure 3A) in addition to the largest drop in TLS efficiency (Figure 2). Many studies indicate a role of pol ζ at the extension step of lesion bypass.[64−67] It therefore seems likely that after insertion of the correct nucleotide dCMP opposite the lesion by one of the Y-family pols, pol ζ preferentially extends the G*:C base pair. In Scheme 2A, we propose a mechanism of error-free TLS, in which pol ζ performs the critical extension step. While the insertion by any of the TLS pols is largely accurate, insertion of a wrong nucleotide also occurs at a substantial frequency. The insertion of a wrong nucleotide, notably dAMP or dTMP, is accomplished by pol η or less frequently by pol ι. Extension of the G*:A or G*:T base pair is most likely conducted by pol κ, as reflected by the most pronounced reduction in MF (Figure 3A) when pol η and pol κ were simultaneously knocked down. A role of Rev1 in mutagenesis is evident from the knockdown experiments, but it does not serve as a deoxycytidyl transferase,[68] as MF decreased dramatically upon Rev1 knockdown (Figure 3A). It may act more effectively as a template for erroneous DNA synthesis by recruiting pol η and pol κ, rather than inserting dCMP opposite the lesion.[69,70] In panels B and C of Scheme 2, we postulate that error-prone TLS is conducted primarily by pol η as the inserter and pol κ as the extender, although pol ι (or pol κ) and pol η, respectively, can act as an inserter and extender, as well, albeit less efficiently. An

dx.doi.org/10.1021/bi5007805 | *Biochemistry* 2014, 53, 5323−5331

Scheme 2. Postulated Pathways of Error-Free and Error-Prone TLS of C8-dG-ABA

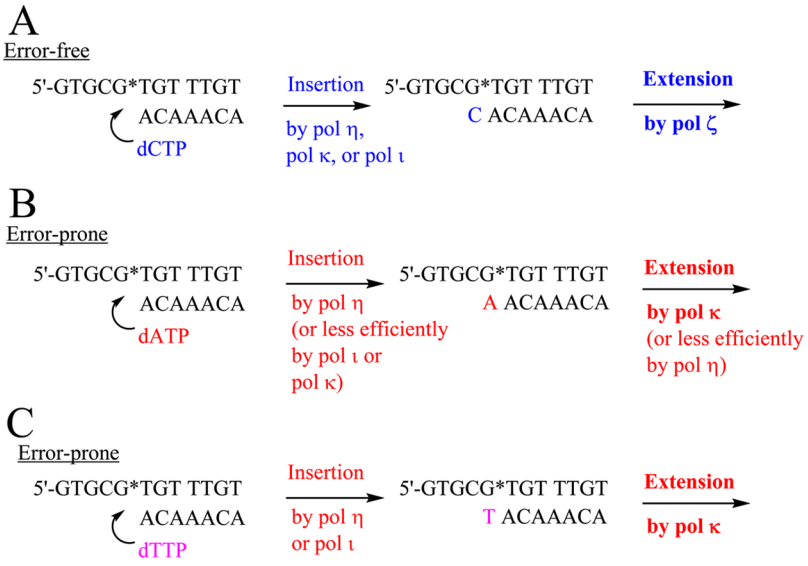

examination of both the percent TLS and MF, as shown in Figures 2 and 3, suggests that when one or more TLS pols are unavailable, the roles of the remaining pols change so that they can at least partially compensate for the absent pols.

Types of Mutations Induced by C8-dG-ABA. The predominant mutation in HEK293T cells was G → T transversion followed by G → A transition. Although there were small differences in the types of mutations in different pol knockdown cells, the pattern of mutations remained comparable in most knockdown experiments (Figure 3B). A noteworthy exception, however, is that in the double-pol knockdown of pol *η* and pol *κ*, pol *η* and pol *ι*, and pol *κ* and pol *ι*, G → A mutations were undetectable. To rationalize this observation, we postulate that insertion of dTMP opposite C8-dG-ABA is accomplished by either pol *η* or pol *ι*, whereas the subsequent extension of the mispair is conducted by pol *κ* (Scheme 2C). Therefore, at least two of these three pols are necessary for G → A mutations. In contrast, dAMP insertion can be conducted by any of the three pols, namely, pol *η*, pol *κ*, or pol *ι*, more efficiently, and extension is executed by either pol *κ* or pol *η* (Scheme 2B). Evidently, additional experiments will be needed to validate these proposed schemes.

The fact that the G → T mutation was the major type of mutation is in stark contrast to another recently reported study in which G → A mutation was the dominant type of mutation.[60] This difference may originate from the differences in the local DNA sequence contexts and the types of cells used. In addition, we used a single-stranded shuttle vector, whereas the reported study was performed in a duplex vector in which the C8-dG-ABA adduct was located in a bubble region.[60] To determine if the bubble region influenced the types of mutations, we replicated a construct in which C8-dG-ABA was placed in a similar bubble. For this experiment, we used COS-7, a different type of mammalian cell line, because we also wanted to determine if mutational types might vary in a dissimilar mammalian cell line. While both the single-stranded and scaffold-containing vector with C opposite the C8-dG-ABA adduct gave similar proportions of G → T and G → A mutations, the frequency of the latter increased dramatically when the adduct was located opposite the bubble scaffold. The mechanism of the change in the mutational specificity when the lesion was located within a bubble is not clear, even though DNA repair may have played a role.

In conclusion, the C8-dG-ABA adduct formed by 3-NBA was found to be mutagenic in human (HEK293T) and simian (COS-7) kidney cells. The major types of mutations were G → T mutations followed by G → A mutations, although G → C and semitargeted mutations also occurred at a low frequency. siRNA knockdown of TLS pols established that each TLS pol, including pol *η*, pol *κ*, pol *ι*, pol *ζ*, and Rev1, played a role in replication across this adduct. Pol *η* and pol *κ* were the major contributors of the mutagenic TLS, but Rev1 was important, as well, presumably performing a noncatalytic role by physically interacting with the other two pols. In contrast, pol *ζ* was involved in the error-free bypass of the lesion.

■ ASSOCIATED CONTENT

Supporting Information

Mass spectra of adducted the 12-mer (Figures S1 and S2), siRNA sequences used for the knockdowns (Table S1), primer sequences used for RT-PCR (Table S2), TLS efficiencies (Table S3), and mutation data (Table S4A–L). This material is available free of charge via the Internet at http://pubs.acs.org.

■ AUTHOR INFORMATION

Corresponding Author

*Department of Chemistry, University of Connecticut, Storrs, CT 06269. E-mail: ashis.basu@uconn.edu. Telephone: (860) 486-3965. Fax: (860) 486-2981.

Funding

This work was supported by National Institute of Environmental Health Sciences Grants ES09127 and ES021762.

Notes

The authors declare no competing financial interest.

■ ABBREVIATIONS

3-NBA, 3-nitrobenzanthrone; C8-dG-ABA, *N*-(2′-deoxyguanosin-8-yl)-3-aminobenzanthrone; N^2-dG-ABA, 2-(2′-deoxyguanosin-N^2-yl)-3-aminobenzanthrone; N^6-dA-ABA, 2-(2′-deoxyadenosin-N^6-yl)-3-aminobenzanthrone; pol, DNA polymerase; TLS, translesion synthesis; HEK, human embryonic kidney.

REFERENCES

(1) Purohit, V., and Basu, A. K. (2000) Mutagenicity of nitroaromatic compounds. *Chem. Res. Toxicol. 13*, 673−692.

(2) Enya, T., Suzuki, H., Watanabe, T., Hirayama, T., and Hisamatsu, Y. (1997) 3-Nitrobenzanthrone, a powerful bacterial mutagen and suspected human carcinogen found in diesel exhaust and airborne particulates. *Environ. Sci. Technol. 31*, 2772−2776.

(3) Suzuki, H., Enya, T., and Hisamatsu, Y. (1997) Synthesis and characterization of some nitrobenzanthrones: Suspected new mutagens in atmospheric environment. *Synthesis*, 1273−1276.

(4) Lamy, E., Kassie, F., Gminski, R., Schmeiser, H. H., and Mersch-Sundermann, V. (2004) 3-Nitrobenzanthrone (3-NBA) induced micronucleus formation and DNA damage in human hepatoma (HepG2) cells. *Toxicol. Lett. 146*, 103−109.

(5) Phousongphouang, P. T., Grosovsky, A. J., Eastmond, D. A., Covarrubias, M., and Arey, J. (2000) The genotoxicity of 3-nitrobenzanthrone and the nitropyrene lactones in human lymphoblasts. *Mutat. Res. 472*, 93−103.

(6) Arlt, V. M., Zhan, L., Schmeiser, H. H., Honma, M., Hayashi, M., Phillips, D. H., and Suzuki, T. (2004) DNA adducts and mutagenic specificity of the ubiquitous environmental pollutant 3-nitrobenzanthrone in Muta Mouse. *Environ. Mol. Mutagen. 43*, 186−195.

(7) Arlt, V. M., Cole, K. J., and Phillips, D. H. (2004) Activation of 3-nitrobenzanthrone and its metabolites to DNA-damaging species in human B lymphoblastoid MCL-5 cells. *Mutagenesis 19*, 149−156.

(8) Arlt, V. M. (2005) 3-Nitrobenzanthrone, a potential human cancer hazard in diesel exhaust and urban air pollution: A review of the evidence. *Mutagenesis 20*, 399−410.

(9) Nagy, E., Zeisig, M., Kawamura, K., Hisamatsu, Y., Sugeta, A., Adachi, S., and Möller, L. (2005) DNA adduct and tumor formations in rats after intratracheal administration of the urban air pollutant 3-nitrobenzanthrone. *Carcinogenesis 26*, 1821−1828.

(10) Arlt, V. M., Bieler, C. A., Mier, W., Wiessler, M., and Schmeiser, H. H. (2001) DNA adduct formation by the ubiquitous environmental contaminant 3-nitrobenzanthrone in rats determined by ^{32}P-postlabeling. *Int. J. Cancer 93*, 450−454.

(11) Bieler, C. A., Arlt, V. M., Wiessler, M., and Schmeiser, H. H. (2003) DNA adduct formation by the environmental contaminant 3-nitrobenzanthrone in V79 cells expressing human cytochrome P450 enzymes. *Cancer Lett. 200*, 9−18.

(12) Bieler, C. A., Cornelius, M. G., Stiborova, M., Arlt, V. M., Wiessler, M., Phillips, D. H., and Schmeiser, H. H. (2007) Formation and persistence of DNA adducts formed by the carcinogenic air pollutant 3-nitrobenzanthrone in target and non-target organs after intratracheal instillation in rats. *Carcinogenesis 28*, 1117−1121.

(13) Seidel, A., Dahmann, D., Krekeler, H., and Jacob, J. (2002) Biomonitoring of polycyclic aromatic compounds in the urine of mining workers occupationally exposed to diesel exhaust. *Int. J. Hyg. Environ. Health 204*, 333−338.

(14) Arlt, V. M., Schmeiser, H. H., Osborne, M. R., Kawanishi, M., Kanno, T., Yagi, T., Phillips, D. H., and Takamura-Enya, T. (2006) Identification of three major DNA adducts formed by the carcinogenic air pollutant 3-nitrobenzanthrone in rat lung at the C8 and N-2 position of guanine and at the N-6 position of adenine. *Int. J. Cancer 118*, 2139−2146.

(15) Arlt, V. M., Zhan, L., Schmeiser, H. H., Honma, M., Hayashi, M., Phillips, D. H., and Suzuki, T. (2004) DNA adducts and mutagenic specificity of the ubiquitous environmental pollutant 3-nitrobenzanthrone in Muta Mouse. *Environ. Mol. Mutagen. 43*, 186−195.

(16) Kawanishi, M., Enya, T., Suzuki, H., Takebe, H., Matsui, S., and Yagi, T. (1998) Mutagenic specificity of a derivative of 3-nitrobenzanthrone in the supF shuttle vector plasmids. *Chem. Res. Toxicol. 11*, 1468−1473.

(17) Cailletfauquet, P., Defais, M., and Radman, M. (1977) Molecular Mechanisms of Induced Mutagenesis: Replication In Vivo of Bacteriophage Phi-X174 Single-Stranded, Ultraviolet Light-Irradiated DNA in Intact and Irradiated Host-Cells. *J. Mol. Biol. 117*, 95−112.

(18) Broyde, S., Wang, L., Rechkoblit, O., Geacintov, N. E., and Patel, D. J. (2008) Lesion processing: High-fidelity versus lesion-bypass DNA polymerases. *Trends Biochem. Sci. 33*, 209−219.

(19) Sale, J. E. (2013) Translesion DNA Synthesis and Mutagenesis in Eukaryotes. *Cold Spring Harbor Perspect. Biol. 5*, a012708.

(20) Ohmori, H., Friedberg, E. C., Fuchs, R. P., Goodman, M. F., Hanaoka, F., Hinkle, D., Kunkel, T. A., Lawrence, C. W., Livneh, Z., Nohmi, T., Prakash, L., Prakash, S., Todo, T., Walker, G. C., Wang, Z., and Woodgate, R. (2001) The Y-family of DNA polymerases. *Mol. Cell 8*, 7−8.

(21) Friedberg, E. C., Wagner, R., and Radman, M. (2002) Specialized DNA polymerases, cellular survival, and the genesis of mutations. *Science 296*, 1627−1630.

(22) Woodgate, R. (1999) A plethora of lesion-replicating DNA polymerases. *Genes Dev. 13*, 2191−2195.

(23) Fuchs, R. P., and Fujii, S. (2013) Translesion DNA Synthesis and Mutagenesis in Prokaryotes. *Cold Spring Harbor Perspect. Biol. 5*, a012682.

(24) Goodman, M. F., and Woodgate, R. (2013) Translesion DNA Polymerases. *Cold Spring Harbor Perspect. Biol. 5*, a010363.

(25) Yang, W., and Woodgate, R. (2007) What a difference a decade makes: Insights into translesion DNA synthesis. *Proc. Natl. Acad. Sci. U.S.A. 104*, 15591−15598.

(26) Makridakis, N. M., and Reichardt, J. K. (2012) Translesion DNA polymerases and cancer. *Front. Genet.* 3 (174), 1−8.

(27) Chandani, S., Jacobs, C., and Loechler, E. L. (2010) Architecture of Y-family DNA polymerases relevant to translesion DNA synthesis as revealed in structural and molecular modeling studies. *J. Nucleic Acids 2010*, No. 784081.

(28) Shachar, S., Ziv, O., Avkin, S., Adar, S., Wittschieben, J., Reissner, T., Chaney, S., Friedberg, E. C., Wang, Z., Carell, T., Geacintov, N., and Livneh, Z. (2009) Two-polymerase mechanisms dictate error-free and error-prone translesion DNA synthesis in mammals. *EMBO J. 28*, 383−393.

(29) Prakash, S., and Prakash, L. (2002) Translesion DNA synthesis in eukaryotes: A one- or two-polymerase affair. *Genes Dev. 16*, 1872−1883.

(30) Johnson, R. E., Washington, M. T., Haracska, L., Prakash, S., and Prakash, L. (2000) Eukaryotic polymerases ι and ζ act sequentially to bypass DNA lesions. *Nature 406*, 1015−1019.

(31) Livneh, Z., Ziv, O., and Shachar, S. (2010) Multiple two-polymerase mechanisms in mammalian translesion DNA synthesis. *Cell Cycle 9*, 729−735.

(32) Ghosal, G., Leung, J. W. C., Nair, B. C., Fong, K. W., and Chen, J. J. (2012) Proliferating Cell Nuclear Antigen (PCNA)-binding Protein C1orf124 Is a Regulator of Translesion Synthesis. *J. Biol. Chem. 287*, 34225−34233.

(33) Yuan, J. S., Ghosal, G., and Chen, J. J. (2012) The HARP-like Domain-Containing Protein AH2/ZRANB3 Binds to PCNA and Participates in Cellular Response to Replication Stress. *Mol. Cell 47*, 410−421.

(34) Dieckman, L. M., and Washington, M. T. (2013) PCNA trimer instability inhibits translesion synthesis by DNA polymerase η and by DNA polymerase δ. *DNA Repair 12*, 367−376.

(35) Kim, H., Dejsuphong, D., Adelmant, G., Ceccaldi, R., Yang, K. L., Marto, J. A., and D'Andrea, A. D. (2014) Transcriptional Repressor ZBTB1 Promotes Chromatin Remodeling and Translesion DNA Synthesis. *Mol. Cell 54*, 107−118.

(36) Park, J. M., Yang, S. W., Yu, K. R., Ka, S. H., Lee, S. W., Seol, J. H., Jeon, Y. J., and Chung, C. H. (2014) Modification of PCNA by ISG15 Plays a Crucial Role in Termination of Error-Prone Translesion DNA Synthesis. *Mol. Cell 54*, 626−638.

(37) Burgers, P. M., Koonin, E. V., Bruford, E., Blanco, L., Burtis, K. C., Christman, M. F., Copeland, W. C., Friedberg, E. C., Hanaoka, F., Hinkle, D. C., Lawrence, C. W., Nakanishi, M., Ohmori, H., Prakash, L., Prakash, S., Reynaud, C. A., Sugino, A., Todo, T., Wang, Z., Weill, J. C., and Woodgate, R. (2001) Eukaryotic DNA polymerases: Proposal for a revised nomenclature. *J. Biol. Chem. 276*, 43487−43490.

(38) Lee, Y. S., Gregory, M. T., and Yang, W. (2014) Human Pol ζ purified with accessory subunits is active in translesion DNA synthesis and complements Pol in cisplatin bypass. *Proc. Natl. Acad. Sci. U.S.A. 111*, 2954−2959.
(39) Yoon, J. H., Prakash, L., and Prakash, S. (2009) Highly error-free role of DNA polymerase η in the replicative bypass of UV-induced pyrimidine dimers in mouse and human cells. *Proc. Natl. Acad. Sci. U.S.A. 106*, 18219−18224.
(40) Washington, M. T., Carlson, K. D., Freudenthal, B. D., and Pryor, J. M. (2010) Variations on a theme: Eukaryotic Y-family DNA polymerases. *Biochim. Biophys. Acta 1804*, 1113−1123.
(41) Schorr, S., Schneider, S., Lammens, K., Hopfner, K. P., and Carell, T. (2010) Mechanism of replication blocking and bypass of Y-family polymerase η by bulky acetylaminofluorene DNA adducts. *Proc. Natl. Acad. Sci. U.S.A. 107*, 20720−20725.
(42) Zhang, Y. B., Yuan, F. H., Wu, X. H., Wang, M., Rechkoblit, O., Taylor, J. S., Geacintov, N. E., and Wang, Z. G. (2000) Error-free and error-prone lesion bypass by human DNA polymerase κ in vitro. *Nucleic Acids Res. 28*, 4138−4146.
(43) Suzuki, N., Ohashi, E., Kolbanovskiy, A., Geacintov, N. E., Grollman, A. P., Ohmori, H., and Shibutani, S. (2002) Translesion synthesis by human DNA polymerase κ on a DNA template containing a single stereoisomer of dG-(+)- or dG-(−)-anti-N^2-BPDE (7,8-dihydroxy-anti-9,10-epoxy-7,8,9,10-tetrahydrobenzo[a]-pyrene). *Biochemistry 41*, 6100−6106.
(44) Avkin, S., Goldsmith, M., Velasco-Miguel, S., Geacintov, N., Friedberg, E. C., and Livneh, Z. (2004) Quantitative analysis of translesion DNA synthesis across a benzo[a]pyrene-guanine adduct in mammalian cells: The role of DNA polymerase κ. *J. Biol. Chem. 279*, 53298−53305.
(45) Liu, Y., Yang, Y. R., Tang, T. S., Zhang, H., Wang, Z. F., Friedberg, E., Yang, W., and Guo, C. X. (2014) Variants of mouse DNA polymerase reveal a mechanism of efficient and accurate translesion synthesis past a benzo[a]pyrene dG adduct. *Proc. Natl. Acad. Sci. U.S.A. 111*, 1789−1794.
(46) Yoon, J. H., Bhatia, G., Prakash, S., and Prakash, L. (2010) Error-free replicative bypass of thymine glycol by the combined action of DNA polymerases κ and ζ in human cells. *Proc. Natl. Acad. Sci. U.S.A. 107*, 14116−14121.
(47) Vasquez-Del Carpio, R., Silverstein, T. D., Lone, S., Johnson, R. E., Prakash, L., Prakash, S., and Aggarwal, A. K. (2011) Role of human DNA polymerase κ in extension opposite from a cis-syn thymine dimer. *J. Mol. Biol. 408*, 252−261.
(48) Nair, D. T., Johnson, R. E., Prakash, S., Prakash, L., and Aggarwal, A. K. (2004) Replication by human DNA polymerase-ι occurs by Hoogsteen base-pairing. *Nature 430*, 377−380.
(49) Nair, D. T., Johnson, R. E., Prakash, L., Prakash, S., and Aggarwal, A. K. (2005) Human DNA polymerase ι incorporates dCTP opposite template G via a G.C plus hoogsteen base pair. *Structure 13*, 1569−1577.
(50) Kirouac, K. N., Basu, A. K., and Ling, H. (2013) Replication of a carcinogenic nitropyrene DNA lesion by human Y-family DNA polymerase. *Nucleic Acids Res. 41*, 2060−2071.
(51) Moriya, M. (1993) Single-stranded shuttle phagemid for mutagenesis studies in mammalian cells: 8-Oxoguanine in DNA induces targeted G.C → T.A transversions in simian kidney cells. *Proc. Natl. Acad. Sci. U.S.A. 90*, 1122−1126.
(52) Gadkari, V. V., Tokarsky, E. J., Malik, C. K., Basu, A. K., and Suo, Z. (2014) Mechanistic Investigation of the Bypass of a Bulky Aromatic DNA Adduct Catalyzed by a Y-family DNA Polymerase. *DNA Repair*, DOI: 10.1016/j.dnarep.2014.06.003.
(53) Pear, W. S., Nolan, G. P., Scott, M. L., and Baltimore, D. (1993) Production of High-Titer Helper-Free Retroviruses by Transient Transfection. *Proc. Natl. Acad. Sci. U.S.A. 90*, 8392−8396.
(54) Hirt, B. (1967) Selective extraction of polyoma DNA from infected mouse cell cultures. *J. Mol. Biol. 26*, 365−369.
(55) Yasui, M., Dong, H., Bonala, R. R., Suzuki, N., Ohmori, H., Hanaoka, F., Johnson, F., Grollman, A. P., and Shibutani, S. (2004) Mutagenic properties of 3-(deoxyguanosin-N2-yl)-2-acetylaminofluorene, a persistent acetylaminofluorene-derived DNA adduct in mammalian cells. *Biochemistry 43*, 15005−15013.
(56) Liu, D., Ryu, K. S., Ko, J., Sun, D., Lim, K., Lee, J. O., Hwang, J. M., Lee, Z. W., and Choi, B. S. (2013) Insights into the regulation of human Rev1 for translesion synthesis polymerases revealed by the structural studies on its polymerase-interacting domain. *J. Mol. Cell Biol. (Oxford, U.K.) 5*, 204−206.
(57) Boiteux, S., and Guillet, M. (2004) Abasic sites in DNA: Repair and biological consequences in *Saccharomyces cerevisiae*. *DNA Repair 3*, 1−12.
(58) Haracska, L., Prakash, L., and Prakash, S. (2002) Role of human DNA polymerase κ as an extender in translesion synthesis. *Proc. Natl. Acad. Sci. U.S.A. 99*, 16000−16005.
(59) Washington, M. T., Minko, I. G., Johnson, R. E., Wolfle, W. T., Harris, T. M., Lloyd, R. S., Prakash, S., and Prakash, L. (2004) Efficient and error-free replication past a minor-groove DNA adduct by the sequential action of human DNA polymerases ι and κ. *Mol. Cell. Biol. 24*, 5687−5693.
(60) Kawanishi, M., Fujikawa, Y., Ishii, H., Nishida, H., Higashigaki, Y., Kanno, T., Matsuda, T., Takamura-Enya, T., and Yagi, T. (2013) Adduct formation and repair, and translesion DNA synthesis across the adducts in human cells exposed to 3-nitrobenzanthrone. *Mutat. Res. 753*, 93−100.
(61) Sale, J. E., Lehmann, A. R., and Woodgate, R. (2012) Y-family DNA polymerases and their role in tolerance of cellular DNA damage. *Nat. Rev. Mol. Cell Biol. 13*, 141−152.
(62) Wu, S., Beard, W. A., Pedersen, L. G., and Wilson, S. H. (2014) Structural comparison of DNA polymerase architecture suggests a nucleotide gateway to the polymerase active site. *Chem. Rev. 114*, 2759−2774.
(63) Wu, W. J., Su, M. I., Wu, J. L., Kumar, S., Lim, L. H., Wang, C. W. E., Nelissen, F. H. T., Chen, M. C. C., Doreleijers, J. F., Wijmenga, S. S., and Tsai, M. D. (2014) How a Low-Fidelity DNA Polymerase Chooses Non-Watson-Crick from Watson-Crick Incorporation. *J. Am. Chem. Soc. 136*, 4927−4937.
(64) Haracska, L., Prakash, S., and Prakash, L. (2003) Yeast DNA polymerase XI is an efficient extender of primer ends opposite from 7,8-dihydro-8-oxoguanine and O-6-methylguanine. *Mol. Cell. Biol. 23*, 1453−1459.
(65) Acharya, N., Johnson, R. E., Prakash, S., and Prakash, L. (2006) Complex formation with Rev1 enhances the proficiency of *Saccharomyces cerevisiae* DNA polymerase for mismatch extension and for extension opposite from DNA lesions. *Mol. Cell. Biol. 26*, 9555−9563.
(66) Xie, Z. W., Braithwaite, E., Guo, D. Y., Zhao, B., Geacintov, N. E., and Wang, Z. A. (2003) Mutagenesis of benzo[a]pyrene diol epoxide in yeast: Requirement for DNA polymerase ζ and involvement of DNA polymerase η. *Biochemistry 42*, 11253−11262.
(67) Guo, D. Y., Wu, X. H., Rajpal, D. K., Taylor, J. S., and Wang, Z. G. (2001) Translesion synthesis by yeast DNA polymerase ζ from templates containing lesions of ultraviolet radiation and acetylamino-fluorene. *Nucleic Acids Res. 29*, 2875−2883.
(68) Nair, D. T., Johnson, R. E., Prakash, L., Prakash, S., and Aggarwal, A. K. (2005) Rev1 employs a novel mechanism of DNA synthesis using a protein template. *Science 309*, 2219−2222.
(69) Guo, C. X., Fischhaber, P. L., Luk-Paszyc, M. J., Masuda, Y., Zhou, J., Kamiya, K., Kisker, C., and Friedberg, E. C. (2003) Mouse Rev1 protein interacts with multiple DNA polymerases involved in translesion DNA synthesis. *EMBO J. 22*, 6621−6630.
(70) Ohashi, E., Murakumo, Y., Kanjo, N., Akagi, J., Masutani, C., Hanaoka, F., and Ohmori, H. (2004) Interaction of hREV1 with three human Y-family DNA polymerases. *Genes Cells 9*, 523−531.